NEUTRAL HYDROGEN IN THE EARTH'S ATMOSPHERE ABOVE 120 KM

BY

MORDEHAI LIWSHITZ

OCTOBER 1965

NASA ———— **GODDARD SPACE FLIGHT CENTER** ————
GREENBELT, MARYLAND

NEUTRAL HYDROGEN IN THE EARTH'S ATMOSPHERE
ABOVE 120 KM

by
Mordehai Liwshitz*

October 1965

*Resident Research Associate – National Academy of Sciences – The National Research Council

Goddard Space Flight Center
Greenbelt, Maryland

SUMMARY

In this paper further results of a study of the neutral hydrogen distribution in the upper atmosphere are presented. These are based on a Monte Carlo calculation of the quasi-stationary neutral hydrogen distribution in the transition region between the collision dominated lower thermosphere and the collisionless exosphere. In this region the rapid loss of fast atoms perturbs the velocity distribution of hydrogen, in effect, cooling the hydrogen relative to the ambient main atmosphere, thereby decreasing the relative loss rate determined by escape. Consequently, under stationary conditions, the hydrogen concentration above the production region is significantly enhanced, leading to a higher hydrogen content in the atmosphere above 120 Km. Results of new calculations of the hydrogen concentration as a function of altitude are presented, as well as the hydrogen content between 120 Km. and various altitudes, for various temperatures of the thermopause, between 1000 and $2500^{\circ}K$. The latter reveal that the "total" hydrogen content of the atmosphere is increased by a factor of ~ 1.1 (at $2500^{\circ}K$) to $\sim .2.0$ (at 1000°). This points to a greater swing in hydrogen content between temperature extrema than that deduced in the convential manner. Both a higher hydrogen content and a greater amplitude of variation with temperature appear to come closer to an explanation of the experimental evidence (mainly Lyman - α radiation). But they also emphasize further the need for a calculation taking into account convection of hydrogen between regions of varying concentration and the effect of the diurnal variation of temperature, which is too fast to permit the establishment of stationary conditions throughout the whole atmosphere.

INTRODUCTION

Though considerable efforts have been spent over the last decade on the elucidation of the problem of hydrogen in the earth's vicinity (see e.g. References 1-3, and the numerous studies cited there) attempts at its solution have met only partial success, and many related observed phenomena still elude a satisfactory quantitative explanation.

Ever since the pioneering rocket experiments on Lyman α radiation by Friedman and co-workers (References 4,5) and the interpretation of their results by Johnson and others (References 6, 7), it had become clear that a sizeable amount of neutral hydrogen, in the order of 10^{13} protons cm^{-2}, is attached to the terrestrial globe, moving with it through the interplanetary medium. This telluric hydrogen corona absorbs, scatters and re-radiates the incoming solar Lyman α radiation, producing the Lyman-α glow observed at high altitudes, both by day and at night. Moreover, its presence is operative in determining the structure of those components of the radiation belts which are sensitive to interaction with neutral hydrogen, such as low energy protons with high pitch angles at relatively great geocentric distances from the equatorial plane (References 8,9).

Though theories of the exosphere (References 2, 10-15) throw considerable light on the variation of the _relative_ hydrogen concentration above 2500 Km, Bates and Patterson (Ref. 16), and Kockarts and Nicolet (References 17-20) were the first to present a detailed picture of the neutral hydrogen distribution throughout the whole atmosphere,

for various temperatures of the thermopause. They recognized that loss of hydrogen incurred from thermal escape leads to a serious departure from diffusive equilibrium in the thermosphere, thereby affecting its vertical distribution at all altitudes. This then results in a strong variation of the atmospheric hydrogen content, from $\sim 5 \times 10^{12}$ atoms cm^{-2} in a column between 1200 and 2000 km, at a thermopause temperature of $1000^\circ K$, to $\sim 1.3 \times 10^{12}$ atoms cm^{-2} at $2000^\circ K$.

This significant advance in the treatment of the problem enabled Thomas and Donahue (Reference 1, References 21-23) to carry through the solution of the difficult radiative transfer problem involved in Lyman-α radiation. Though the results of these calculations are indicative of the basically correct approach of the authors quoted in the last paragraph, some difficulties were left unresolved which mar somewhat the validity and applicability of the hydrogen atmosphere model proposed by them.

It provided no satisfactory quantitative explanation of the observed intensity variation with solar zenith angle, nor could the required optical depths, which are proportional to the hydrogen content above 120 Km, be satisfactorily reconciled with the atmospheric conditions, mainly temperature, prevailing when the Lyman α radiation was observed.

Though these difficulties are related to the time-dependent asymmetry of the hydrogen corona, and the associated lateral flow (References 24, 25), we first address ourselves to a problem which appears of basic importance even in the time-independent treatment of a symmetric hydrogen atmosphere. As Nicolet points out (Reference 20), one cannot accept a Maxwellian distribution as representing real conditions at the base of the exosphere. One might also add that the concept of a fixed,

temperature independent critical level at ~ 500 Km, underlying the
calculations in References 16-20 might have to be discarded, in view of
the considerable variation in the number density of the main constituents
at this altitude, which may change by about an order of magnitude, say,
between thermopause temperatures of 800 and 1200^OK (Reference 26).

In a previous paper (Reference 27), a method was described to
evaluate the hydrogen velocity distribution in the vicinity of the critical
level, which takes account of the non-equilibrium situation, brought about
by thermal evaporation. Preliminary results for thermopause temperatures
of 1500 and 2500^OK were also presented, indicating that the relative escape
rate of hydrogen is, indeed, reduced quite significantly. As pointed out
there, the reduction is greater than deduced in earlier attempts (References
2, 28, 29) at solving the escape problem, since at no point in our calcu-
lations any particular form of the velocity distribution was introduced
in the calculation.

The basic idea underlying our method was the division of the upper
atmosphere into three regions, and can best be visualized with the aid of
the schematic model in Fig. 1: lowermost is the bulk of the thermosphere,
where solution of the Chapman-Cowling diffusion equation (Reference 30)
appears adequate in deducing the vertical distribution of hydrogen. Next
we evaluate the evolvement of the quasi-steady-state hydrogen distribution
in an extended transition region by means of the Monte Carlo method. The
uppermost region is the exosphere, where again conventional methods may
be applied. In a sense the two upper regions overlap partially, since we
place the critical level, the exobase, ˜ some distance below the top of
the transition region, where the Monte Carlo calculation is carried out.

This procedure then serves to take some account of the occurence of collisions in the exosphere, rare though they are, and eliminates spurious effects resulting from the sharp artificial boundary at the top. This boundary bears the character of a semi permeable membrane reflecting slow atoms, but passing those above escape velocity. For further details of the method, and the underlying shochastic model our previous paper may be consulted.

In this present note additional results for thermopause temperatures of 1000 and 2000°K are presented, as well as the results of a new calculation of the steady-state hydrogen atmosphere above 120 km, based on the Monte Carlo results. In these calculations all three methods described in the last paragraph were applied, each in its appropriate range.

The Monte Carlo results in the transition region for thermopause temperatures of 1000 and 2000°K fit in well with the earlier results. Those for 2000°K yielded values of the significant parameters (effusion velocity, response time of the hydrogen distribution to abrupt changes in temperature, concentration gradients etc.) intermediate between those of the bracketing temperatures of 1500° and 2500°K. The results for 1000°K also appear to be consistent with these, though in the latter case the statistical accuracy of the effusion velocity, $\sim 2 \times 10^2$, is rather poor.

Again, as in the earlier results, interpretation of the dispersion of the various velocity components as effective temperatures of the hydrogen, displays the "anisotropic cooling" effect, observed there.

This interpretation appears to be quite useful in the evaluation of the hydrogen distribution in the exosphere. The relative concentration in the exosphere derived from the raw Monte Carlo data on angular and velocity

- 4 -

distribution at the exobase differs only by at most 10% from the values obtained for an equivalent exosphere computed in the conventional manner from a Maxwellian distribution of hydrogen at the base, whose temperature is lower than that of the ambient oxygen, assumed in diffusive equilibrium. It appears that the _relative_ concentration in the exosphere is reduced at large distances by a factor of 2-4, depending on temperature. In the light of the cooling effect discussed, this reduction follows from the reduced hydrogen scale height caused by the lower temperature.

The _absolute_ concentration in the exosphere, however, is determined by the concentration at the critical level which has to be obtained by deducing the concentration profile of hydrogen throughout the thermosphere. This has been done by solving the diffusion problem in this region in a manner similar to that first proposed by Mange (Reference 31), and applied since in the calculations of References 16-20. We have used the Harris and Priester model atmospheres (Reference 26) as the medium through which hydrogen diffuses upward.

Finally, the three separate portions of the concentration profile were combined and the concentration profile of hydrogen above 120 Km was obtained, for the four thermopause temperatures considered. Integration of the concentration curves between 120 Km, and higher altitudes yields then the hydrogen content between these two layers.

Since Harris and Priester (Reference 26) base their models on constant boundary conditions at 120 Km, while Kockarts and Nicolet (References 17-20) use constant boundary conditions at 100 Km, we have carried out corresponding calculations based on the diffusion velocities derived from Jeans' formula.

This permits comparison between the profiles obtained when the effect of escape on the hydrogen velocity distribution is taken into account, and those deduced in the convential manner.

The important results from this comparison are as following: in the thermosphere the concentration of neutral hydrogen is effectively closer to diffusive equilibrium than convential escape theory predicts, while the converse holds in the exosphere, a consequence of the cooling effect discussed. Overall, because of the reduced relative escape rate, and the ensuing prolonged sojourn of hydrogen atoms in the atmosphere, concentrations are, in general, higher than obtained hitherto, except at large distances, in the order of 4 earth radii. Consequently, for the same rate of supply by the source of atomic hydrogen from photo-dissociation of water vapor and methane (Reference 31), the atmosphere has a higher hydrogen content, than predicted hitherto.

If we assume an average concentration of $10^6 cm^{-3}$ hydrogen atoms at 120 KM, the respective values of the hydrogen content in a $1 cm^2$ column above this level are $\sim 1.37 \times 10^{13}$ cm^{-2} at $1000^\circ K$ and 2.00×10^{12} cm^{-2} at $2500^\circ K$, as compared to 6.9×10^{12} cm and 1.79×10^{12} cm^{-2} at the corresponding temperatures, when the conventional loss rates are applied. More details can be inspected from the curves in the following sections.

These results suggest higher optical depths for Lyman α, and predict a greater swing of the hydrogen content than assumed up to now. Though this appears to be in the right direction (see e.g. Reference 1, References 21, 22), it even more stresses the need for a comprehensive time dependent treatment of the problem.

FURTHER RESULTS OF THE MONTE CARLO CALCULATION
ON THE HYDROGEN DISTRIBUTION IN THE TRANSITION REGION

In this section the results of additional Monte-Carlo computations of the hydrogen distribution in the transition region are represented, and some general conclusions are drawn from these results. Since the procedure applied was identical to that reported in a previous communication (Reference 27), and so are the definitions of some relevant quantities, this should be referred to for details.

As was done there, the atmospheric parameters used in the computation are based mainly on the work of Harris and Priester (Reference 26), and are summarized in Table 1.

TABLE 1

ATMOSPHERIC PARAMETERS USED IN THE
COMPUTATION FOR THE 1000° AND 2000°K
CASES

Atmospheric Temperature ($^{\circ}$K)	Altitide (Km)	Oxygen Concentration (cm^{-3})	Mean Free Path (Km)	Scale Height (Km)
1000	320	3.5×10^{8}	10.54	62.5
	580	5.5×10^{6}	670.00	
2000	500	2.32×10^{8}	19.5	112.0
	950	4.20×10^{6}	1080.0	

Again, as in the previous work, the limits of _physical_ validity, i.e. the boundaries of the _physical transition region_ between thermosphere and exosphere, are taken at the lower end where the slope of the M.C. curve approaches that of an approximate diffusive equilibrium curve, while at the top the exospheric base ($\lambda = 2.5H$) is assumed to bound it.

The part of the density curve obtained from the Monte Carlo computation in the transition region is represented by the beaded portion of the solid curves in Figures 1 and 2, extending between 300 and 480 Km., respectively 520 and 800 Km for the two additional cases treated. As in the previously reported cases, also included in these figures, there is an inflexion in these curves, which reflects the closer approximation to diffusive equilibrium in the lower thermosphere, compared to conventional calculations, whereas toward the exosphere the departure from equilibrium is more pronounced.

Figure 4 represents the response or relaxation times of the layers near the critical level. These can be seen to vary inversely to temperature between ~ 1300 sec. to 1000°K to ~ 650 sec. at 2500°K. They can best be interpreted as characteristic times for the establishment of stationary conditions in the velocity distribution of hydrogen in the transition region, while the response of the concentration will be determined to a considerable extent by the altered vertical and lateral diffusive flux into the region.

This effectively means that the change in relative effusion velocities, shown in Figure 5, will lag behind the change in temperature approximately proportional to $e^{-t/T}$; while the change in the absolute loss rate will vary in a more complicated way.

Now, with respect to the relative reduction in effusion velocity, compared to values derived via Jeans formula, it has alreay been observed in our previous paper that this reduction is greater for the lower thermopause temperatures, in the range considered, than for higher ones. Some reflection may convince us that this result is not quite so surprising as one might be tempted to think at first.

It is quite clear that Jeans' formula furnishes upper limit values for thermal escape (see e.g. Reference 33). Consider now the hypothetical case of zero temperature. Evidently there is no thermal escape whatsoever, neither as derived from Jeans' formula for $E \rightarrow \infty$, nor from a hypothetical Monte Carlo calculation, if this were possible. Thus we may assume that at very low temperatures the two curves for the effusion velocity approach each other.

On the other hand consider a relatively high temperate T. Let us consider the maximum geocentric distance R_m attainable by hydrogen atoms of mass m and mean energy $3kT/2k$ where k is the Boltzmann constant. From concervation of energy we obtain

$$3kT/2 - mg(R_o) R_o = -mg(Rm)Rm \tag{1}$$

$$= -mg(R_o) R_o^2 / Rm$$

where R_o is, say, the geocentric distance of the vertical level, and g the gravitational acceleration. Then

$$Rm = R_o E/(E-1.5) \tag{2}$$

where E is the escape parameter of $(R_o) R_o/kT$. Equation (2) means that once E reaches a value of 1.5, eventually all hydrogen will escape from the atmosphere. Thus escape will be very fast, and the two effusion velocity curves will again intersect. This is illustrated by the extrapolation of the Monte Carlo curve beyond the computed value for 2500 k. In between there is a region of maximum departure of the real effusion velocity from the Jeans effusion velocity. This seems to be located towards the lower thermopause temperatures in the range considered here.

Moreover, we may also consider the cooling effect discussed above. In a first approximation let us assume that the fractional decrease in hydrogen temperature, T eff, at the critical level is proportional to the ambient thermopause temperature, T_∞, i.e.

$$T_{eff} = T_\infty \ (1-\alpha) \tag{3}$$

If we apply Jeans' formula, we obtain for the ratio, R_v, between the effective effusion velocity, and the Jeans effusion velocity

$$R_v = (1-\alpha)^{\frac{3}{2}} \ [1+E/(1-\alpha)] \ e^{-\frac{\alpha E}{1-\alpha}} \ /(1+E) \tag{4}$$

If we take $\alpha \sim 0.2$, we obtain for hydrogen in the terrestrial atmosphere the values of R_v given in Table 2, as a function of temperature.

TABLE 2

R_v, Ratio of Effective to Equilibrium Effusion Velocity

T ($^\circ$K)	E	R_v
1000	7.05	.265
1500	4.64	.423
2000	3.26	.552
2500	2.77	.606
3000	2.31	.658
4000	1.73	.729
4500	1.54	.814

Again we observe that the relative effect is more pronounced at lower temperatures, in agreement with our computational results.

Figure 6 represents the effective temperature of hydrogen at the critical level as a function of the thermopause temperature. This is defined here as the geometric mean between the critical effective temperature and the omnidirectional effective temperature, defined in Reference 27. The rationale in applying this particular averaging method was the desire to take some account of the geometry of the actual problem, whereas the computations

were carried out in plane geometry. <u>After</u> these averages were taken

it was found that the exospheric distributions decuced with these tempera-

tures yield an almost perfect fit to those obtained from the raw data of

the Monte Carlo computation.

It is seen that in the range of our computations the effective temperature

lies about 25% below the ambient thermopause temperature. We believe

this effect to be real, and consider it to be the combined effect of both

the rapid escape of fast particles, as well as some loss of speed by

fast hydrogen atoms in collision with oxygen, since collisions are not

frequent enough to bring about detailed balance. If there were some heating

of the ambient oxygen it would be too minute to produce any observeable

effects. The extrapolation of the effective temperature curve beyond

the computed values is of a tentative character. Beyond $T_\infty \sim 4500°K$ (E~1.5)

escape presumably becomes so fast that the concept of temperature may no longer

be meaningful.

Though no Figures are shown here, representing the "microscopic"

results, such as angular and velocity distributions for 1000 and 2000°K,

these bear the same character as those of the earlier results for 1500 and

2500° which are amply illustrated in the earlier paper (Reference 27).

THE RELATIVE CONCENTRATION OF HYDROGEN IN THE
EXOSPHERE

The relative concentration of an atmospheric constituient in the exosphere may be evaluated, once its velocity distribution at the critical level is known. The latter is defined by Öpik and Singer as the level where

$$H n \sigma \sim 0.5 \qquad\qquad (5)$$

Here H denotes the real height of effective atmospheric number density (i.e. that of oxygen in our case); n_0 is the effective number density at the leval, and σ an effective collision cross section.

A more precise averaging method used by us does not materially change this criterion. If the angular probability density of the upward flux is given by $2x\,dx$ (with x the zenith angle cosine), the condition for a collision probability of $\frac{1}{2}$ in the upward omnidirectional flux is

$$2 \int_0^1 e^{-H/\lambda_0 x}\, x\, dx = .5 \qquad\qquad (6)$$

changing to a variable $\xi = H/\lambda$, one obtains

$$e^{-\xi} - \xi e^{-\xi} - \xi^2 Ei(-\xi) = \tfrac{1}{2} \qquad\qquad (7)$$

then $Ei(-\xi)$ is the exponential integral

$$-Ei(-\xi) = \int_\xi^\infty \frac{e^{-t}}{t}\, dt$$

Equation (7) has a solution $\xi \sim 0.4$ in fair agreement with Equation (5). Applying this criterion we obtained with the aid of the atmospheric data used altitudes of 480, 580, 800, and 900 Km for the altitude of the critical level at respective thermopause temperatures of 1000, 1500, 2000 and 2500°K.

In the Monte Carlo computation we obtained the required velocity distributions for hydrogen in the form of two dimensional arrays g_{ij}, essentially histograms of the population of thin layers (5-10 Km thick. Here the first subscript, i, refers to one of the 20 equal intervals in (-1, 1), the range of direction angle cosines, while the second subscript, j, refers to one of the 50 intervals in speed between 0 and $10kT\infty/m$, the latter varying from $\sim$ 40 Km/sec at 1000°K to $\sim$ 64.3 Km/sec at 2500°K. To facilitate computation in the exosphere the "vectors" g_{ij} for any particular value of i were numerically approximated by a least square method by functions

$$j_i(v) = A_i v^2 e^{-\beta_i v^2} \tag{8}$$

A goodness of fit test was applied to the approximations thus obtained. As observed in our previous paper the distributions obtained are quite symmetrical (though not isotropic) in x, the zenith angle cosine, up to $v\infty$. The relative concentration at an inverse geocentric distance $y=R_o/R$ may then be represented by a sum of integrals (similar to the double integral in References 11 or 14)

$$\rho(Y) = y^2 \Sigma_i \mu_i F_i(\mu_i, y) \tag{9}$$

where
$$\rho(Y) = n_h(R)/n_h(R_o)$$
$$\mu_i = \langle x_i \rangle$$

a mean value of x in the ith interval, and

$$F_i(\mu_i, y) = \int\limits_{v\,min\,(\mu_2, y)}^{\infty} fi(v_1) \left\{ v^2[1-y^2(1-\mu_i^2)]-v_\infty^2(1-y) \right\}^{-\frac{1}{2}} v^3 \, dv$$

$$+ \int\limits_{v\,min\,(\mu_i, y)}^{+} fi(v) \left\{ v^2[1-y^2(1-\mu_i^2)]-v_\infty^2(1-y) \right\}^{-\frac{1}{2}} v^3 dv \qquad (10)$$

$v_{min}(\mu_2, y)$ is obtained from conservation of energy in orbital motion, as

$$v_{min} = v_\infty^2(1-y)/[1-y^2(1-\mu^2)] \qquad (11)$$

To test the dependence of the exospheric distribution on the exact choice of the escape level - and this is important in our study since we do not use an exact Maxwellian distribution there - we carried out the calculation of Equation (9) with the values for F_i obtained from the arrays g_{ij} in two nearby layers, $\sim$ 50 Km apart, near the "exact" escape level. The resultant exospheric concentrations were almost identical everywhere within $\sim$ 3% of each other.

In a similar manner exospheric concentrations were derived by using at the escape level Maxwellian distributions appropriate to the effective temperatures represented in Figure 6, which also closely approximated the curves for the Monte Carlo derived exosphere.

These curves are shown in Figures 7 and 8. Figure 7 illustrates the decrease in relative hydrogen concentration versus R/Re, where Re is the earth's radius. The dashed curves represent the variation in number density obtained from Maxwellian distributions at the respective ambient thermopause temperatures. To complete the picture, curves for the corresponding barometric distributions are inserted. As can be seen, the difference between the set of solid curves and the dashed ones increases quite rapidly with increasing geocentric distance; but the ratio between the concentrations approaches fairly constant values at around 10 earth radii.

This can be seen more clearly in Figure 8, where this ratio R_n is plotted versus $S = R-R_o/H_h$, which appears a more suitable parameter for comparison of results for different temperatures. Here H_h is the hydrogen scale height.

As with the effusion velocity, the effect on the exosphere is more pronounced at lower temperature, the ratio R_n at large distances varying from about 0.25 for $1000^{\circ}K$ to about 0.6 at $2500^{\circ}K$. Again the explanation is that a roughly constant _fractional_ decrease in the temperature at the critical level is more effective due to the exponential factor $e^{-(R-R_o)/H}$, which enters into most calculations.

We have included Figure (9) showing the passage from the transition region to the exosphere. These curves represent relative hydrogen concentration versus S, normalized to unity at the assumed escape level. The beaded portion of the curve is obtained from the Monte Carlo calculation, while the solid portion shows the exospheric results discussed in this section. The region of overlap has been mentioned before, and has no physical significance beyond partial consideration of the rare encounters in the exosphere.

THE ABSOLUTE CONCENTRATION OF HYDROGEN ABOVE 120 Km.

A knowledge of the relative variation of concentration in the transition region and the exosphere is of limited practical value unless the absolute concentration at some level can be estimated. To do this, one has to calculate the concentration profile through out the thermosphere, down to the vicinity of the production region, where a more or less reliable estimate of absolute concentration can be attempted (References 17, 32).

In doing so we proceeded in a manner similar to that applied by Bates and Patterson (Reference 16), starting with the equation of continuity

$$n(R)w(R)R^2 = S_a R_a^2 \qquad (12)$$

Here w denotes the net flow velocity of hydrogen at R S_a is the specific loss rate of hydrogen at a level R_a, considered in the following as the upper boundary for our computation. We choose R_a at a level within the transition region, where the slope of the concentration profile approaches diffusive equilibrium. From there downward we feel justified in using Chapman's expression for the diffusion velocity (Reference 30, Equation 14.1.1)

$$w = - \frac{n^2}{n_h n_o} D_{Ho} \left\{ \frac{d}{dR} \left(\frac{n_h}{n} \right) + \frac{n_h n_o}{n\rho} (m_o - m_n) \frac{\partial \log P}{\partial R} + k_T \frac{1}{T} \frac{\partial T}{\partial R} \right\} \qquad (13)$$

Here $n_h \, cm^{-3}$ is the hydrogen concentration, $n_o \, cm^{-3}$ stands for the concentration of main atmospheric constituents - mainly atomic oxygen close to the transition region, and molecular nitrogen near 120 Km.

D_{Ho} is the binary diffusion coefficient for the O-H mixture, $n = n_H + n_o$, m and m_o are the respective masses of hydrogen and an average over the main constituents, p is the pressure, T the temperature, k_T is the thermal diffusion ratio.

In this scalar form Equation 13 accounts only for radial flow, corresponding to a spherically symmetric steady state model of the atmosphere. Now since $n_h \ll n_o$, Equation 13 reduces to

$$w = -D_{Ho} \left\{ \frac{1}{n_h} \frac{dn_h}{dR} - \frac{1}{n} \frac{dn}{dR} + \frac{d\log p}{dR} - \frac{m}{m_o} \frac{1}{p} \frac{dp}{dR} + \alpha_T \frac{dT}{dR} \right\} \quad (14)$$

where α_T is the thermal diffusion factor, $\alpha_T \sim K_T \, n/n_h$,

Since

$$p = nKT \quad (15)$$

$$\frac{d\log p}{dR} = \frac{1}{n} \frac{dn}{dR} + \frac{1}{T} \frac{dT}{dR} \quad (16)$$

whence

$$w = -D_{HD} \left\{ \frac{1}{n_h} \frac{dn_h}{dR} + (1 + \alpha_T) \frac{d\log T}{dR} - \frac{m}{m_o} \frac{d\log p}{dR} \right\} \quad (17)$$

Let $z = R_\rho - R$ $(R < R_\rho)$ such that Equation (12) becomes

$$w(R) = \frac{\mathcal{E}_a}{n(R)} \left(\frac{R_a}{R_a - z} \right)^2 \quad (18)$$

This may now be combined with Equation (17) to yield

$$\left[\frac{d}{dz} + (1+\alpha_T) \frac{d\log T}{dz} - \frac{m_H}{m} H^{-1} \right] n_h = \frac{\mathcal{E}_a}{D_{12}(z)} \left(\frac{R_a}{R_a - z} \right)^2 \quad (19)$$

where H is the local pressure scale height

$$H = \left(\frac{1}{p} \frac{dp}{dz} \right) \quad (20)$$

Let $P(z) = \int_0^z \left[(1 + \alpha_T) \frac{d\log T}{dz} - \frac{m_H}{mH} - dz \right]$ $\quad (21)$

which may be used for an integration factor to obtain a solution of Equation (19) in the form

$$n_h(z) = n_h(0) \left\{ (T_o/T_z)^{(1+\alpha_T)} e^{Q(z')} \left[1 + \int_0^z \phi(z', e^{P(z')} dz') \right] \right\} \quad (22)$$

where

$$Q(t) = m \int_{o}^{t} \frac{dt^{1}}{Hm} \tag{23}$$

and

$$\phi(t') = \frac{S_a}{D_{Ho}} \left(\frac{R_a}{R_\rho - t} \right)^{2} \tag{24}$$

D_{Ho}^{-1} was approximated by the hard sphere formula

$$D_{Ho}^{-1} = \frac{8}{3} n_o(z) \pi \sigma^2 \sqrt{\frac{2}{\pi}} \left[\frac{mm_o}{(m+m_o)KT} \right]^{\frac{1}{2}} \tag{25}$$

Numerical evaluation of Equation (21) yields the concentration of hydrogen below R_a, relative to that at R_a. In the actual numerical work use was made of Harris and Priester's model atmosphere (Reference 26). Specifically the following tabulations were applied at the respective thermopause temperatures:

$1000^{\circ}K$	Model 5,	00 hrs.
$1500^{\circ}K$	Model 8,	08 hrs.
$2000^{\circ}K$	Model 10,	12 hrs.
$2500^{\circ}K$		extrapolation

If one considers the relative concentration, assuming $n(R_a)=1$, S_a becomes numerically equal to the net flow velocity at R_a. To permit comparison Equation 21 was integrated twice for each thermopause temperature, once using a value $S_a(M.C)$ based on the Monte Carlo result, while for the second calculation a value $S_a(M.B.)$ derived from Jeans' formula was substituted. Table 3 presents the respective values of Z_o, S_a, R_a and R_o, the assumed altitudes of the critical levels for the various temperatures

TABLE 3

VALUES OF R_a, S_a, AND R_o FOR VARIOUS TEMPERATURES T_∞

$T_\infty(^\circ K)$	R_a (Km)	Z_o (Km)	S_a (M.C.)(cm^2 sec^{-1})	S_a (M.B.)cm^{-2} sec^{-1}
1000	6770	480	1.80×10^2	7.56×10^2
1500	6830	580	1.85×10^3	6.45×10^3
2000	6970	800	5.05×10^3	1.70×10^4
2500	6970	900	1.20×10^4	2.99×10^4

For α_T a mean value of -0.2 was taken from Reference 33. Equation 21 was calculated from the respective level R_a downward to 120 Km, where the concentration of the various atmospheric constituents is constant, in accordance with the Harris-Priester model (Reference 16).

Since we are interested in absolute concentrations, the hydrogen concentration at this level was assumed to be 10^6 cm^{-3}. Estimating the hydrogen diffusion velocity there as ~ 2.5 cm sec^{-1} this gives a source flux of $\sim 2.5 \times 10^7$ cm^{-2} sec^{-1}, in agreement with Nicolet's earlier estimates (Refs. 17, 31, and 32). The three independent portions of the concentration profile were then combined and are presented in Figures 2, 3, 10 and 11. Solid curves are based on the M.C. results, the portion with solid circles being obtained directly from the Monte Carlo calculation in the transition layer, whereas the portion with open circles represents the exospheric distribution based on the former. Dashed curves represent the concentration profile based on the conventional treatment of escape.

As a comparison of the two sets of curves indicates, what we believe to be the real hydrogen concentration profile above 120 Km is actually overall closer to diffusive equilibrium than a profile derived with the aid of Jeans' formula. This strengthens our contention that on a large scale escape perturbs the medium less than application of the former indicates.

Consistently the Monte Carlo concentration curves lie higher than the corresponding alternate curves, except at large distances $(\sim 4R_\rho)$ where the curves approach each other or even intersect. This is easier to accept than the converse; loss from escape should affect the concentration more at high altitudes than in the thermosphere at large kinetic depths below the escape level.

Inspection of the curves reveals that the difference between the corresponding concentrations reaches a maximum in the vicinity of the critical level, where the assumed sink is located. The ratio of the corresponding concentrations is in the order of ~ 3, closely related to the ratio of the corresponding effusion velocities.

Of greater interest in direct relation to some observed phenomena than the concentration itself is its integral, $\int_{z_1}^{z_2} n(z)dz$, between two specific limits, yielding the total hydrogen content between these two layers. Numerical integration of $n(z)$ has been performed by us, the resulting curves being shown in Figures   and   .

These confirm our expectation that the hydrogen content per cm^2, $N_n^{(z)} \int_{120}^{z} n(z')dz'$, between 120 Km and higher levels (z) is considerably enhanced due to the smaller relative loss rate, as compared to results obtained in the conventional manner.

Both in absolute numbers, and relatively, this enhancement is more pronounced at lower thermopause temperatures than at higher ones. This is indicated in Table 4, where the "total hydrogen content per cm^2, $\int_{120}^{\infty} n(z)dz$ is presented both from the Monte Carlo results as well as from the conventional calculation. Moreover their ratio R_n is given, and the ratio

$N_\infty(T)/N_\infty(1000)$ of the total content at a thermopause temperature $T^\circ K$ to that at $1000^\circ K$.

TABLE 4

TOTAL HYDROGEN CONTENT cm^{-2} AND VARIOUS RATIOS FOR DIFFERENT
THERMOPAUSE TEMPERATURES

| $T_\infty(^\circ K)$ | $N_\infty(T)$ cm^{-2} | | R_n | $N_\infty(T)/N_\infty(1000$ | |
	M.C.	M.B.		M.C.	M.B.
1000°	1.34×10^{13}	6.9×10^{13}	1.94	1.00	1.00
1500°	4.13×10^{12}	2.36×10^{12}	1.75	0.309	0.342
2000°	2.60×10^{12}	1.89×10^{12}	1.38	0.194	0.274
2500°	2.00×10^{12}	1.78×10^{12}	1.12	0.149	0.258

Of special interest in these results is the greater amplitude in the variation of the total hydrogen content cm^{-2} with temperature. Though it cannot be assumed that the full swing of this variation can be realized on a diurnal scale, as will be discussed in the last section of our paper, it certainly predicts a larger difference in the hydrogen content between periods of high and low solar activity. This actually may be even greater than the above numbers indicate, since the latter are based on constant boundary conditions at 120 Km, while the actual situation may allow for some variation of hydrogen concentration even at this low level (see e.g. Reference 18).

CONCLUSIONS

The results of this new investigation of the steady state neutral hydrogen distribution above 120 Km presented here indicate that thermal escape is less effective in disturbing the diffusive equilibrium of hydrogen in the thermosphere than was previously assumed, whereas, on the other hand, its effect on the distribution of hydrogen in the exosphere is stronger than thought hitherto.

Consequently, in view of the smaller relative escape rate the overall hydrogen content of the atmosphere is enhanced by a factor of ~ 1.1-2.0 in the range of thermopause temperatures considered here. From the trend indicated in the variation of this factor it is likely that the relative enhancement may be in the order of ~ 2.5 for the range of temperature prevailing near solar minimum, which appears to be about 600-800°K.

It should be noted, however, that the difference between the present model and previous ones is not great enough to permit on the basis of available experimental data an unequivocal decision with respect to its fundamental correctness.

Indications of evidence in its favor appear to be the following: The present results can more easily provide the required optical depths called for a satisfactory explanation of Lyman $\sim \alpha$ experiments. (References 21-23, References 34, 35). These require the presence of up to $\sim 4 \times 10^{13}$ hydrogen atoms cm^{-2} above 120 Km, which can be well accounted for by our model, without stretching the source requirements unduly beyond 2.5×10^{7} cm^{-2} sec^{-1}.

It appears easier, for instance, to deduce from our model the con-
centrations used by Donahue (Reference 23) in his interpretation of the
Javelin rocket experiment (Reference 36), carried out in January 1960.
These were $\sim 9 \times 10^4$ cm^{-4} and 5×10^4 cm^{-3} at altitudes of 500 and 1100 Km
respectively. The thermopause temperature assumed by Donahue was 1000°K,,
which appears 10-15% too low (e.g. Ref. 37), such that the concentration
at 1000 Km would have to be increased even above the high value of 3×10^7
cm^{-3} quoted by him. To yield the required concentrations, at the higher
altitudes, 2×10^7 cm^{-3} hydrogen atoms at the 100 Km level would suffice
in our model.

Nonetheless, our steady state model suffers from the inherent defect
of all such models. In view of the even wider swing in the total hydrogen
content with varying temperature it is hard to reconcile the required supply
of hydrogen in sufficiently short time (10 hours) to make up for the
vast difference in the steady state abundance between day time and night
time temperatures. This is so, notwithstanding the fact that the relative
distribution in the transition region displays relatively very short response
times, in the order of an hour or less. But the difference between the
content cm^{-2} between, say 1500° and 1100° (corresponding to conditions
during the winter of 1959-60) is in the order of 5×10^{12} cm^{-2}, while the
assumed source yield is $\sim 2.5 \times 10^7$ cm^{-2}sec^{-1} half a day. This is short of
the required quantity by almost an order of magnitude. Consequently the
full swing between the steady state abundances corresponding to diurnal
temperature extrema will never be fully realized.

This has been recognized by Hanson et al (Reference 24), in their study of diurnal variations (Reference 24). Their conclusion that the day time temperature determines the mean diurnal concentration appears, however, questionable in view of the observed wide variation in day time concentrations (Reference 35); the relative variation of hydrogen abundance is greater at lower temperatures.

Though their treatment of lateral flow was an important start, conclusions from their and later attempts by Donahue and McAfee (Reference 25) have not yet sufficiently clarified to what extent the lateral diffusion of hydrogen is effective in limiting the diurnal variation. It appears that no satisfactory picture of the hydrogen profile in the geocorona can be obtained, before a time dependent, three dimensional model is investigated without neglect of transport in the thermosphere.

Such an investigation may, for instance, throw light on the following effect: While transport in the thermosphere and near the critical level tends to reduce the diurnal difference in hydrogen content cm^{-2}, this reduction may be limited in the exosphere. At some distance from the earth the nocturnal exosphere derives actually from day time hydrogen near the critical level (and vice versa). As a result of the latter's higher temperature it falls of less sharply than would be expected from night time temperatures.

ACKNOWLEDGEMENTS

REFERENCES

1. DONAHUE, T. M. and THOMAS, G., Planet. Space Sci. 10, 65, (1963).

2. CHAMBERLAIN, J. W., Planet. Space Sci. 11, 901, (1963).

3. KURT, V. G., Soviet Phys. Usp., 6, 701, (1964) (Transl. from Russian).

4. BYRAM, E. T. et al. The Threshold of Space, pp. 203-209, Pergamon Press, London (1957).

5. KUPPERIAN, J. E. et al, Planet. Space Sci. 1, 3, (1959).

6. JOHNSON, F. S., Tech. Rep. LMSD 49719, Lockheed Aircraft Corp., (1959).

7. JOHNSON, F. S. and FISH, R. A., Ap. J. 131, 502 (1960).

8. NAKADA, M. P. and MEAD, G.D., Tech. Rep. X-640-65-273, GSFC, (1965).

9. CORNWALL, J. M. et al., J. Geoph. Res. 70, 3099 (1965).

10. ÖPIK, E. J. and SINGER, S. F., Phys. Fluids, 2, 653, (1959).

11. ÖPIK, E. J. and SINGER, S. F., Phys. Fluids, 3, 483, (1969).

12. ÖPIK, E. J. and SINGER, S. F., Phys. Fluids, 4, 221, (1961).

13. JOHNSON, F. S., Ap. J., 133, 701 (1960).

14. HERRING, J. and KYLE, L., J. Geophys. Res. 66, 1980 (1961).

15. AMODT, R. E. and CASE, K. M., Phys. Fluids 5, 1019 (1962).

16. BATES, D. R. and PATTERSON, T.N.L., Planet Space Sci. 5, 257 (1961).

17. KOCKARTS, G. and NICOLET, M., Ann. Geophys., 18, 269 (1962).

18. KOCKARTS, G. and NICOLET, M., Ann. Geophys., 19, 370 (1963).

19. NICOLET, M., Geophysics, The Earth's Environment, pp. (Gordon and Breach, N.Y. and London) (1963).

20. NICOLET, M., Research in Geophysics, 1, pp. 243-275, (The M.I.T. Press, Cambridge, Mass.) (1964).

21. THOMAS, G. E., J. Geophys. Res. 68, 2639, (1963).

22. DONAHUE, T.M. and THOMAS, G. E., J. Geophys. Res. 68, 2661, (1963).

23. DONAHUE, T. M., J. Geophys. Res. $\underline{69}$, 1301, (1964)

24. HANSON, W. B. and PATTERSON, T.N.L., Planetary Space Sci., $\underline{11}$, 1035, (1963).

25. DONAHUE, T.M. and McAfee, J.R., Planetary Space Sci. $\underline{12}$, 1045, (1964)

26. HARRIS, I. and PRIESTER, W., Report on the Atmospheric Structure in the Region from 120 Km to 800 Km, Cospar, Buenos Aires, May 1965.

27. LIWSHITZ, M., and SINGER, F. S., NASA Tech. Note, G-645, (1965).

28. BIUTNER, E. K., Soviet Astronomy AJ $\underline{2}$, 528, (1958) (Transl. from Russian).

29. BIUTNER, E. K., Soviet Astronomy AJ ($\underline{3}$, $\underline{92}$, (1959) (Transl. from Russian).

30. CHAPMAN, S., and COWLING, T. G., "The Mathematical Theory of Non-Uniform Gases," 2nd ed., Cambridge Univ. Press, 1952.

31. MANGE, P., Ann. Geophys. $\underline{17}$, 277, (1961).

32. BATES, D. R. and NICOLET, M., J. Geophys. Res., $\underline{55}$, 301, (1950).

33. KRUPENIE, P. H. and al., J. Chem. Phys., $\underline{39}$, 2399, (1963).

34. DONAHUE, T. M. and FASTIE, W. G., Space Research IV, pp. 304-324, (Nort Holland Pub. Co., Amsterdam 1964)

35. DONAHUE, T. M., paper presented at Aeronomy Symposium, Cambridge, Mass., Aug. 1965 (unpublished).

36. CHUBB, T. A. et al., Mem. Soc. Roy. Sci. Liege, $\underline{4}$, 437, (1961)

37. NICOLET, M., J. Geophys. Res., $\underline{68}$, 6121, (1963).

COLLISIONLESS
EXOSPHERE

SEMI PERMEABLE
BOUNDARY

EXOBASE $\lambda \geq 2.5$ H

EXTENDED ISOTHERMAL
TRANSITION LAYER
PREDOMINANTLY OXYGEN

PERMEABLE BOUNDARY
$\lambda_H \ll H$

COLLISION DOMINATED
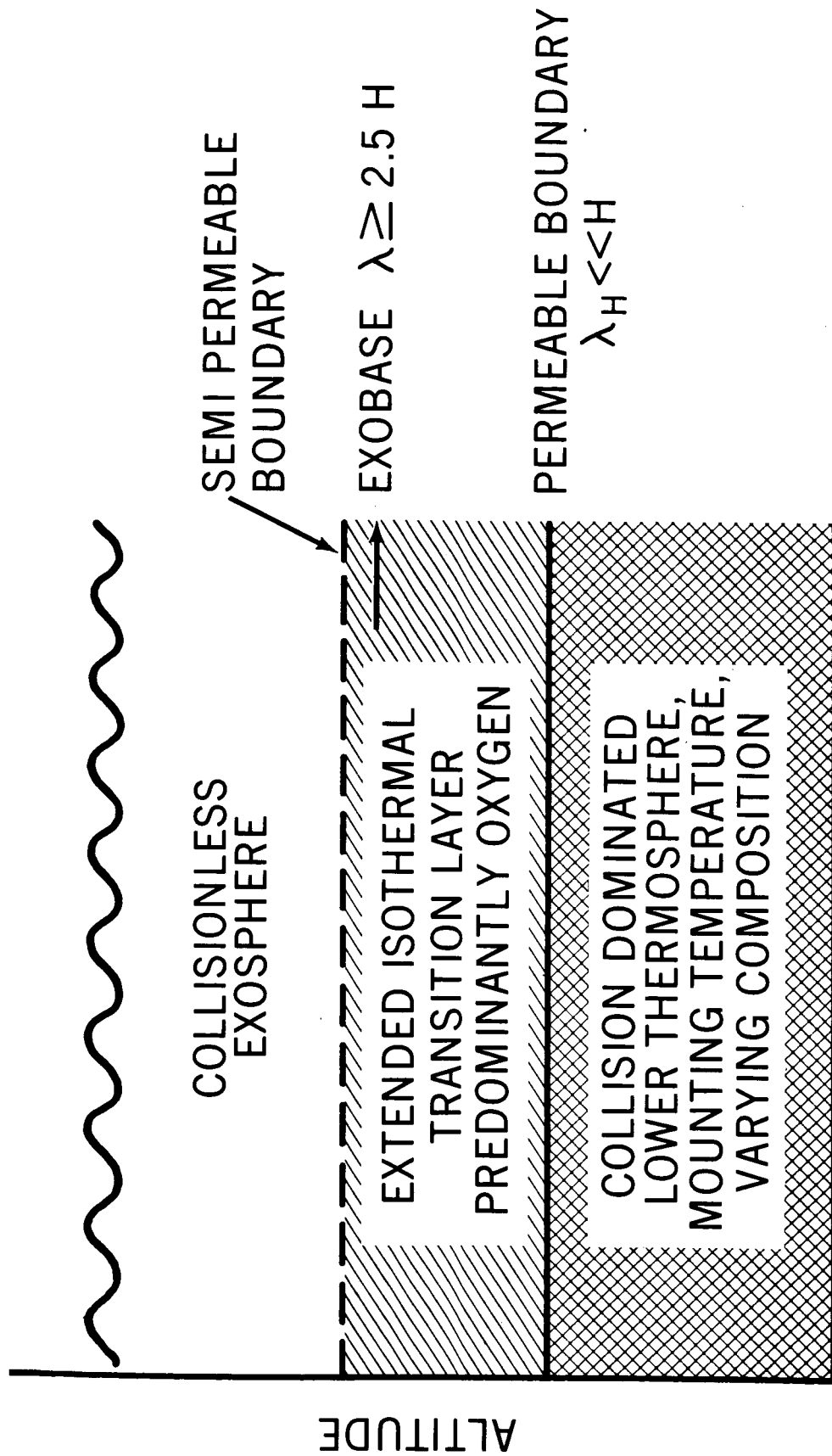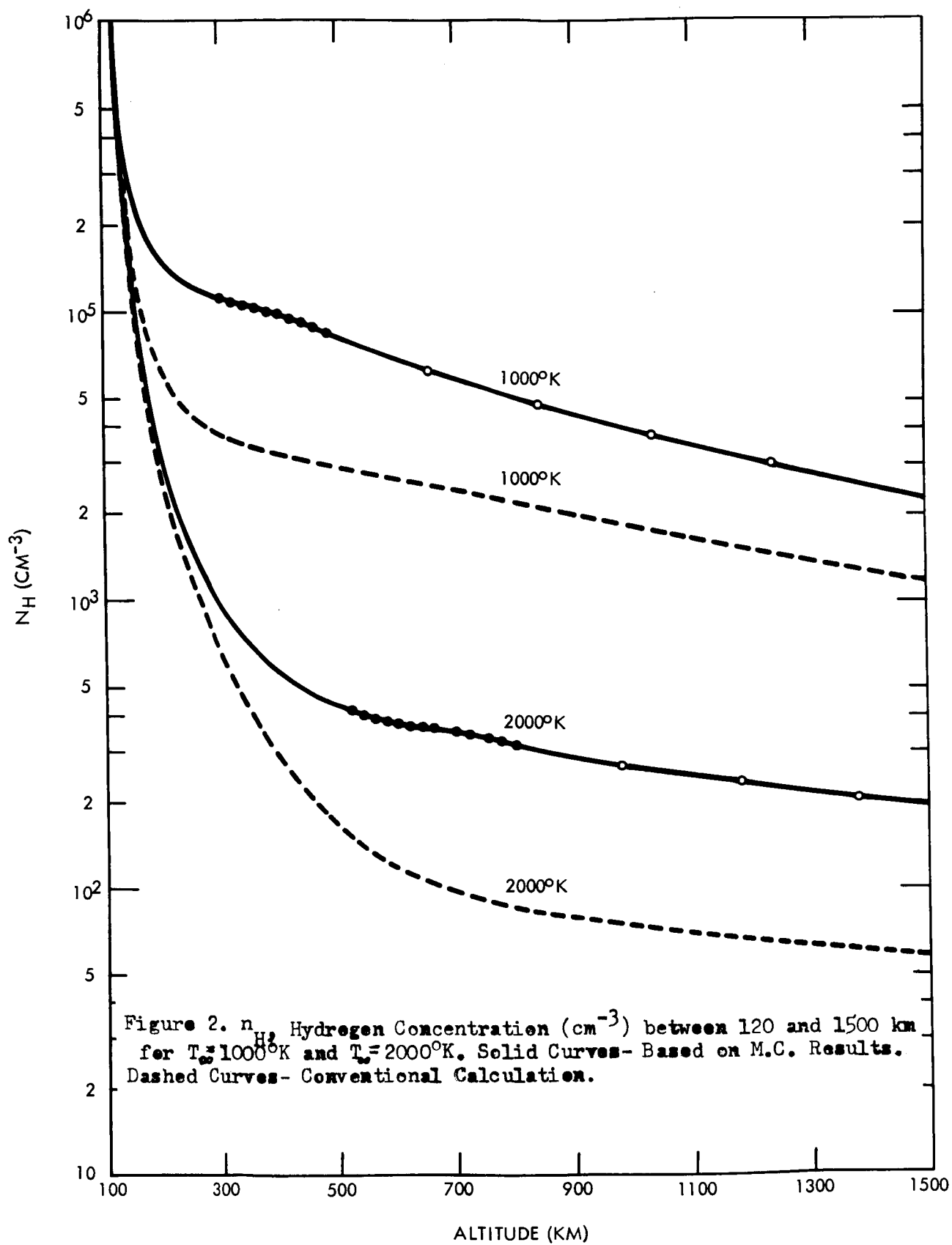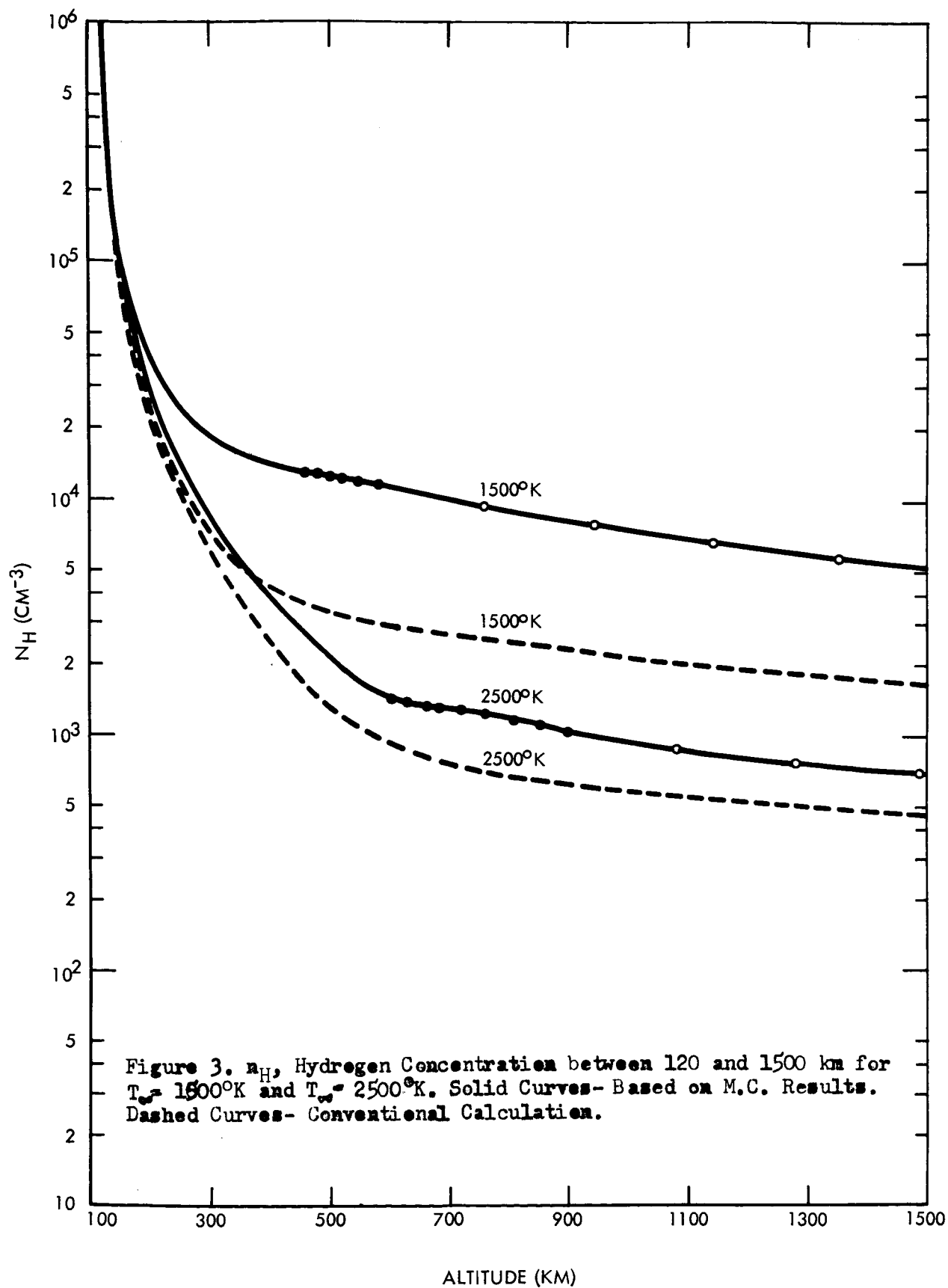LOWER THERMOSPHERE,
MOUNTING TEMPERATURE,
VARYING COMPOSITION

ALTITUDE

Figure 1. Schematic Model of the Upper Atmosphere.

Figure 2. n_{H}, Hydrogen Concentration (cm^{-3}) between 120 and 1500 km for T_{∞}=1000°K and T_{∞}=2000°K. Solid Curves- Based on M.C. Results. Dashed Curves- Conventional Calculation.

Figure 3. n_H, Hydrogen Concentration between 120 and 1500 km for $T_\infty = 1500^\circ K$ and $T_\infty = 2500^\circ K$. Solid Curves- Based on M.C. Results. Dashed Curves- Conventional Calculation.
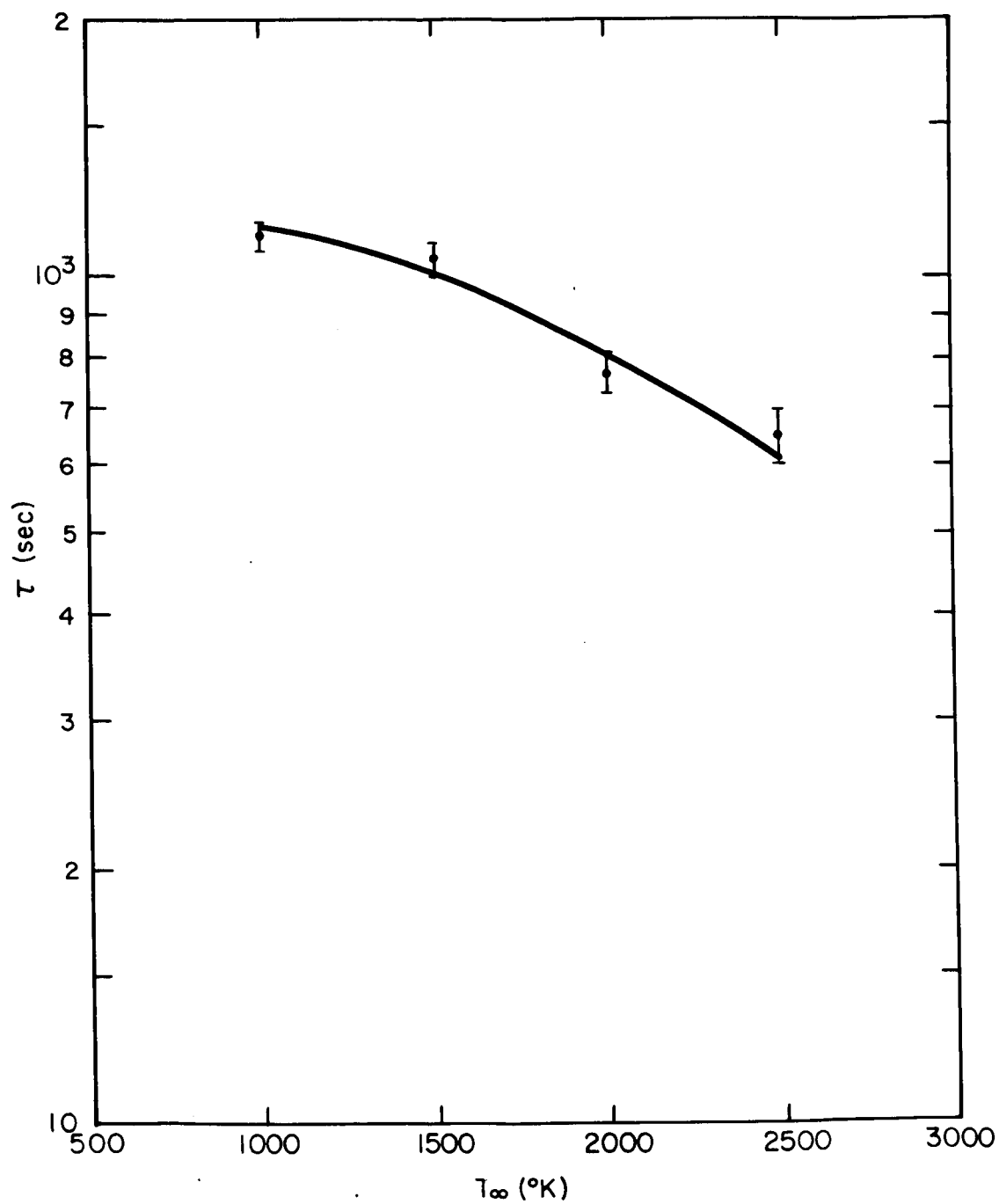
Figure 4. Response Time Near the Critical Level vs. Thermopause
Temperature.

Figure 5. V_E, Effusion Velocity vs. Thermopause Temperature T_∞. Solid Curve- Monte Carlo Results. Dash- Dot Curve- Extrapolation of M.C. Results. Dashed Curve- from Jeans' Formula.
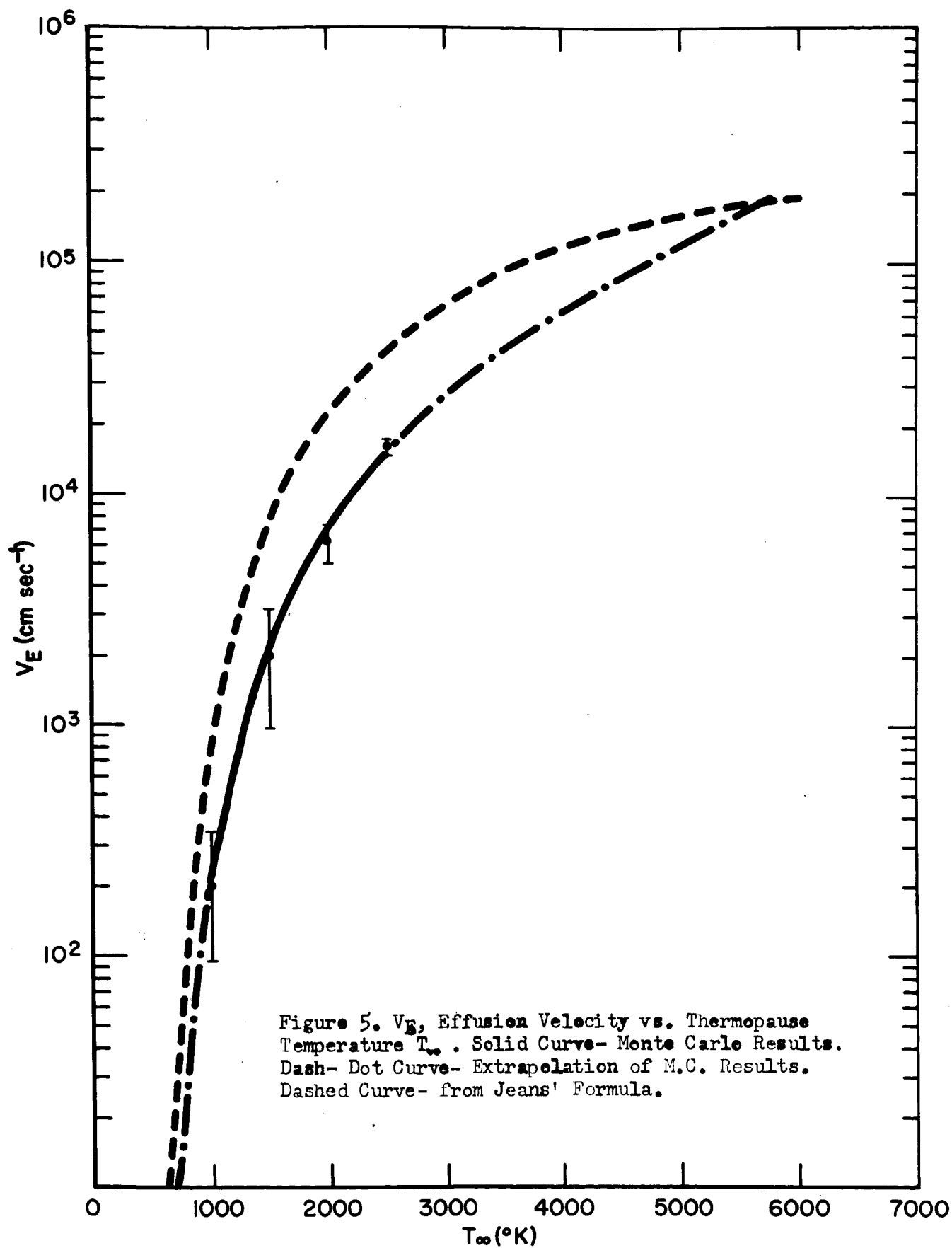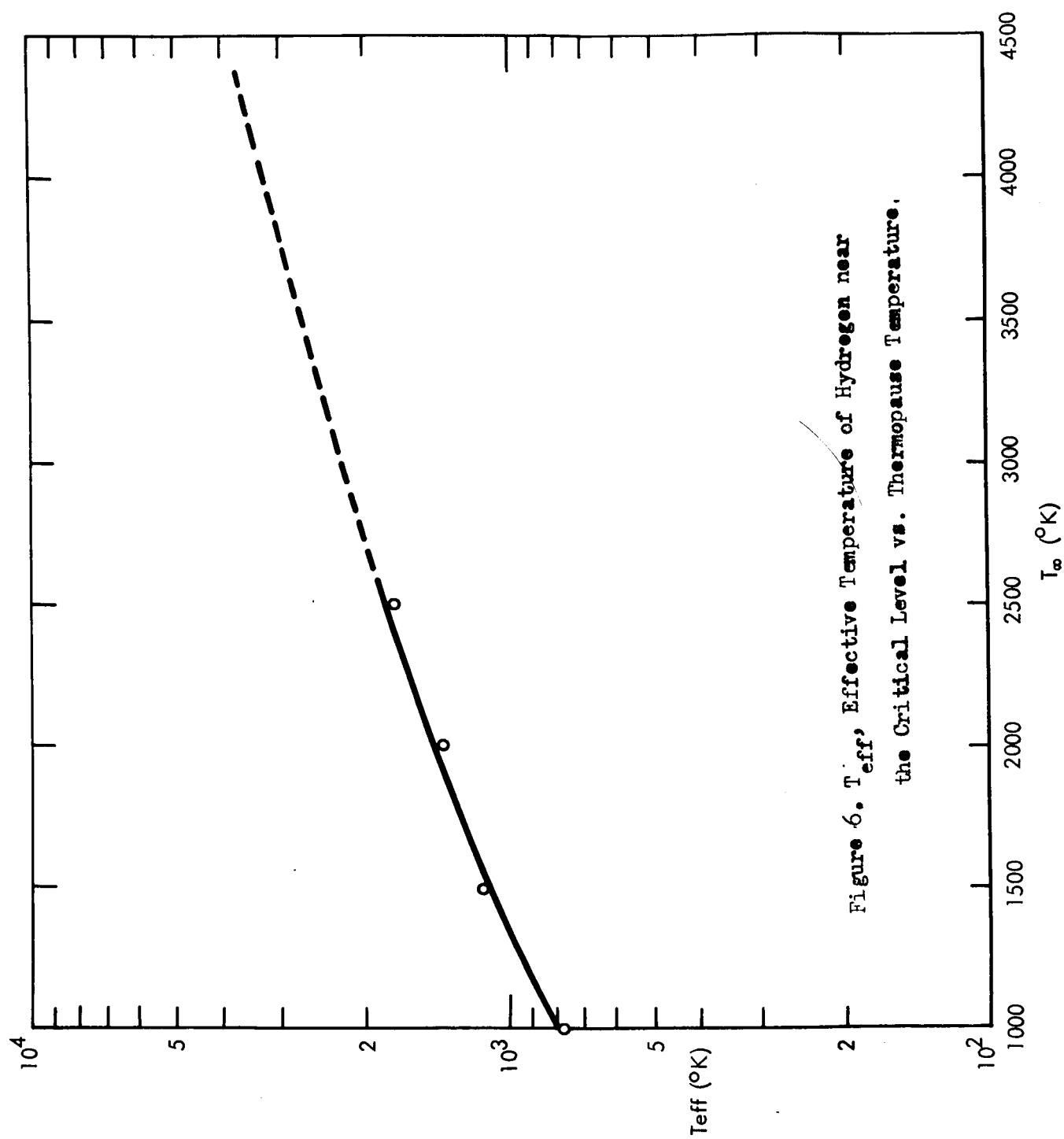
Figure 6. T_{eff}, Effective Temperature of Hydrogen near the Critical Level vs. Thermopause Temperature.
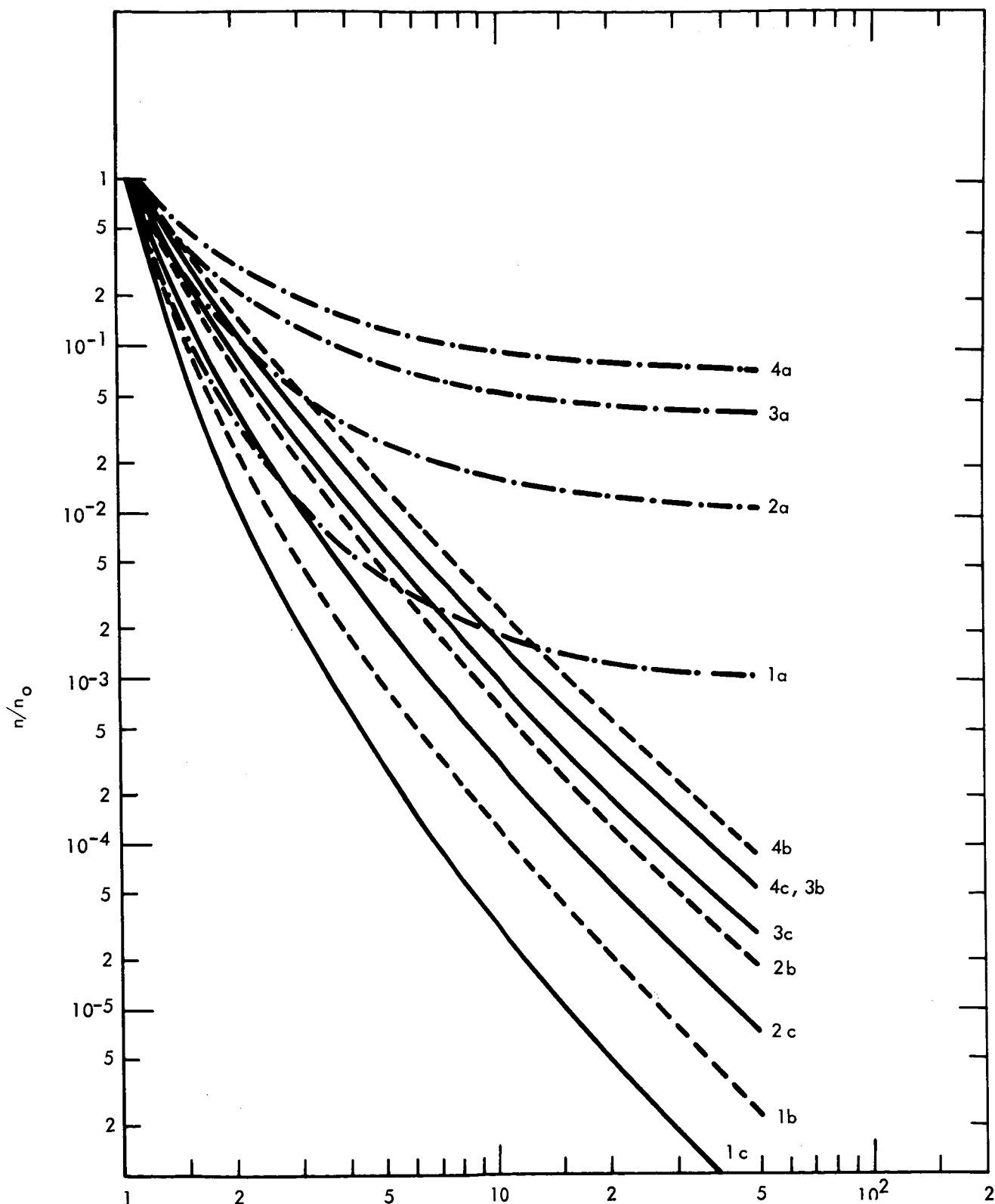
Figure 7. n/n_o, Relative Hydrogen Concentration in the Exosphere vs. Geocentric Distance (in Units of Earth Raddi) for Various Values of T . Numbers 1,2,3,4 Refer to 1000°, 1500°, 2000°, 2500°K Respectively. Letters a,b,c Refer to the Barometric Formula, the Conventional Exospher and an Exosphere based on the M.C. Results.
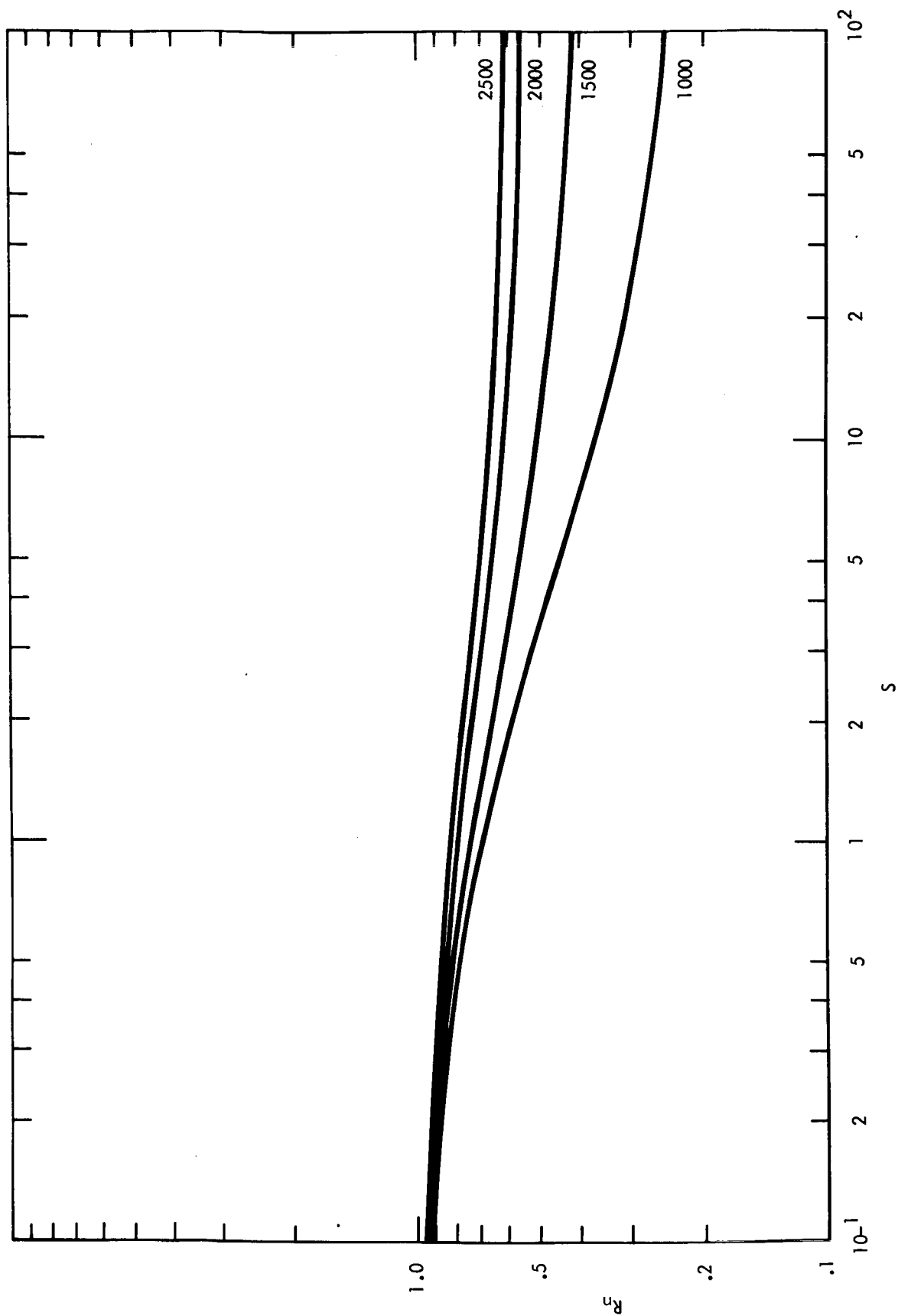
Figure 8. R_n, Ratio of Exospheric Hydrogen Concentrations Derived from M.C. Results to Concentrations Derived from Conventional Theory, vs. $s = (r-r_o)/H_o$, for Various $T\infty$.
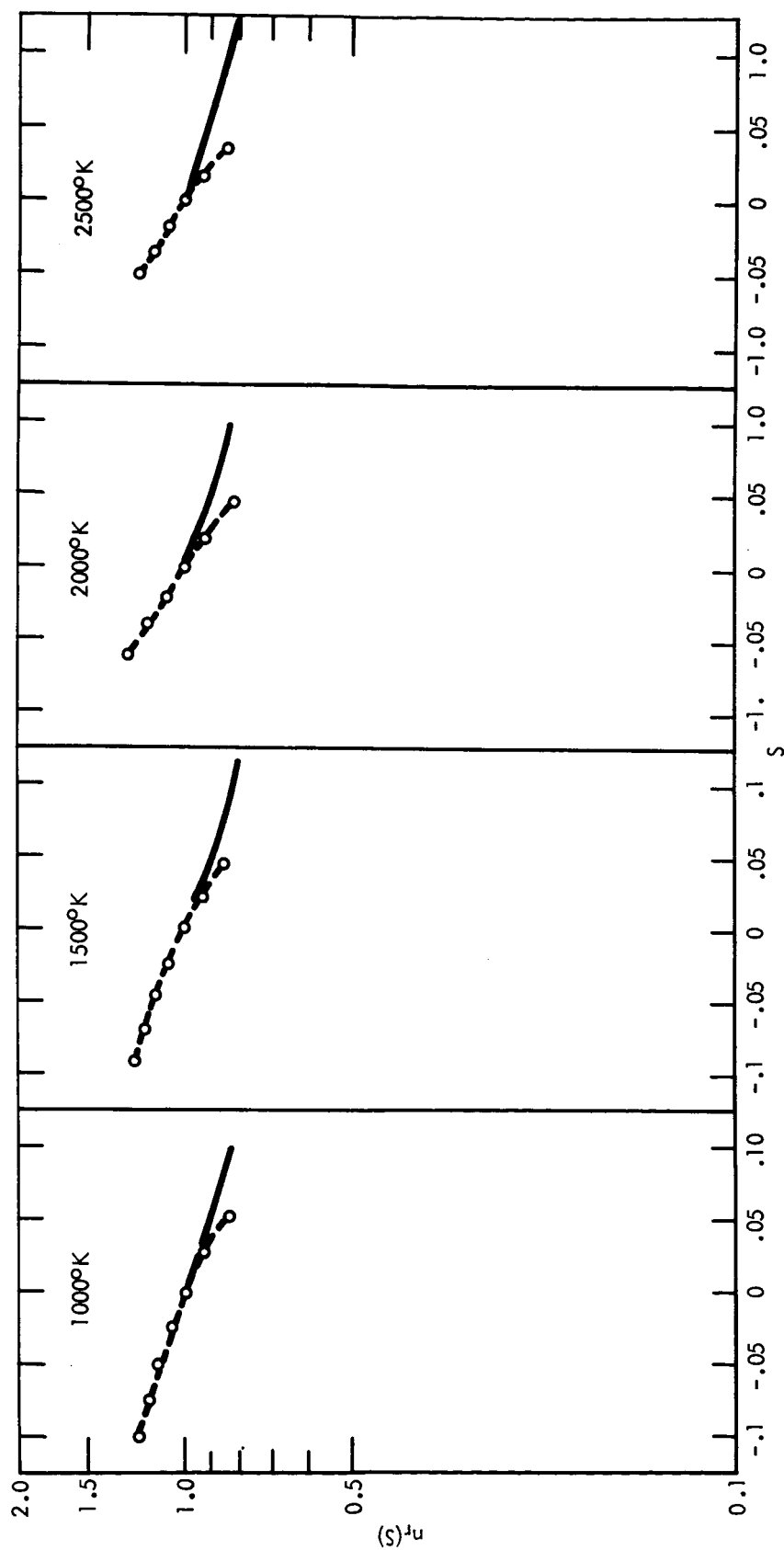
Figure 9. Passage from Transition Region to Exosphere for Various Values of $T\alpha$. 0 is the Assumed Critical Level. $n_r(s) = n_H(s\delta)/n_H(0)$. $s = z/H_0$.
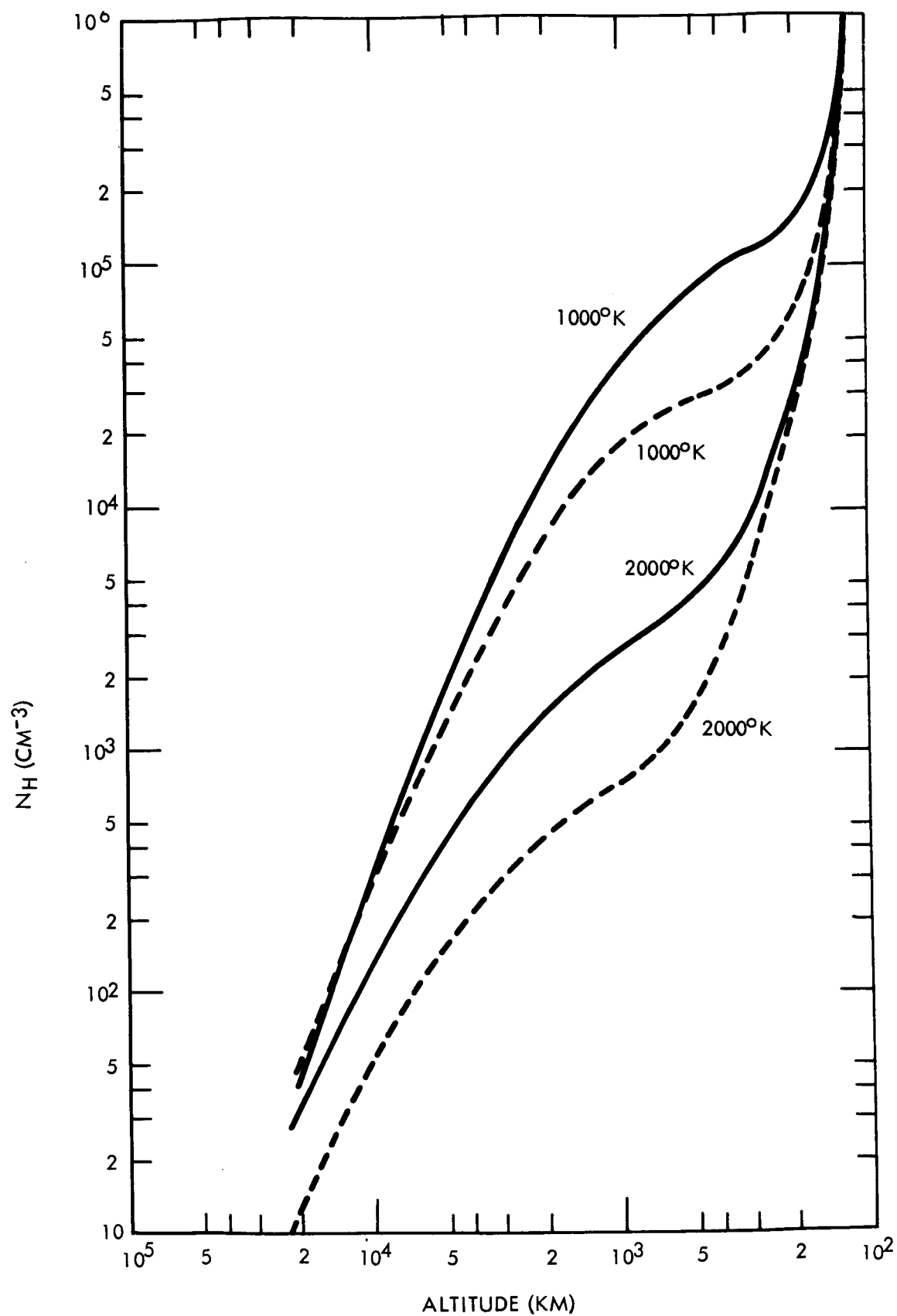
Figure 10. N_H, Hydrogen Concentration (cm^{-3}) vs Altitude above 120 km for $T \approx 1000^{\circ}K$ and $T \approx 2000^{\circ}K$. Solid Curves- Based on M.C. Results. Dashed Curves- Conventional Calculation.
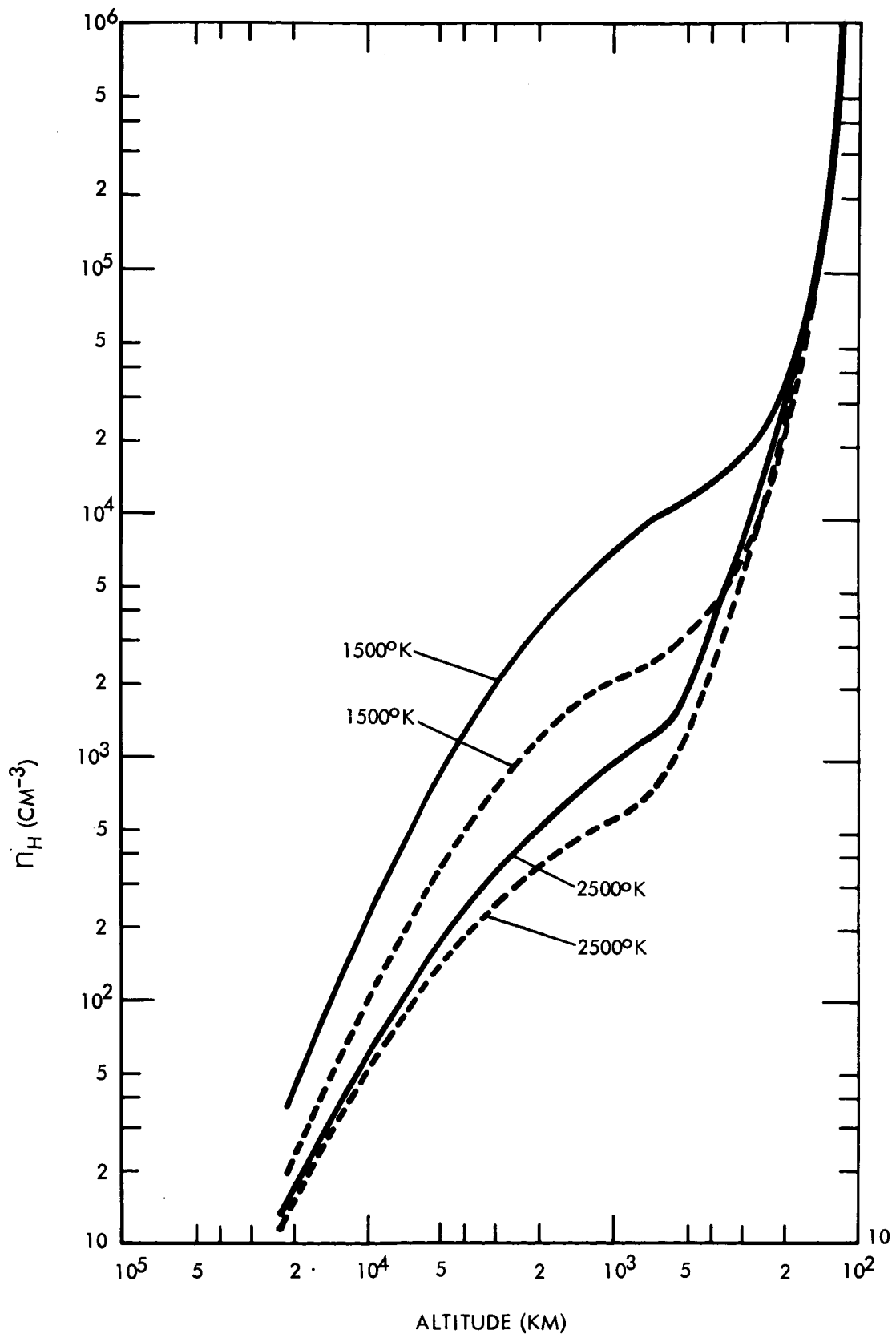
Figure 11. n_H, Hydrogen Concentration (cm^{-3}) vs. Altitude above 120 km, for $T_\infty = 1500°K$ and $T_\infty = 2500°K$. Solid Curves , Based on M.C. Results. Dashed Curves- Conventional Calculation.

Figure 12. N_H, Number of HydrogenAtoms per cm^2 above 120 km, for $T_v = 1000^\circ K$ and $T_v = 1500^\circ K$. Solid Curves- Based on M.C. Results. Dashed Curves- Conventinal Calculation
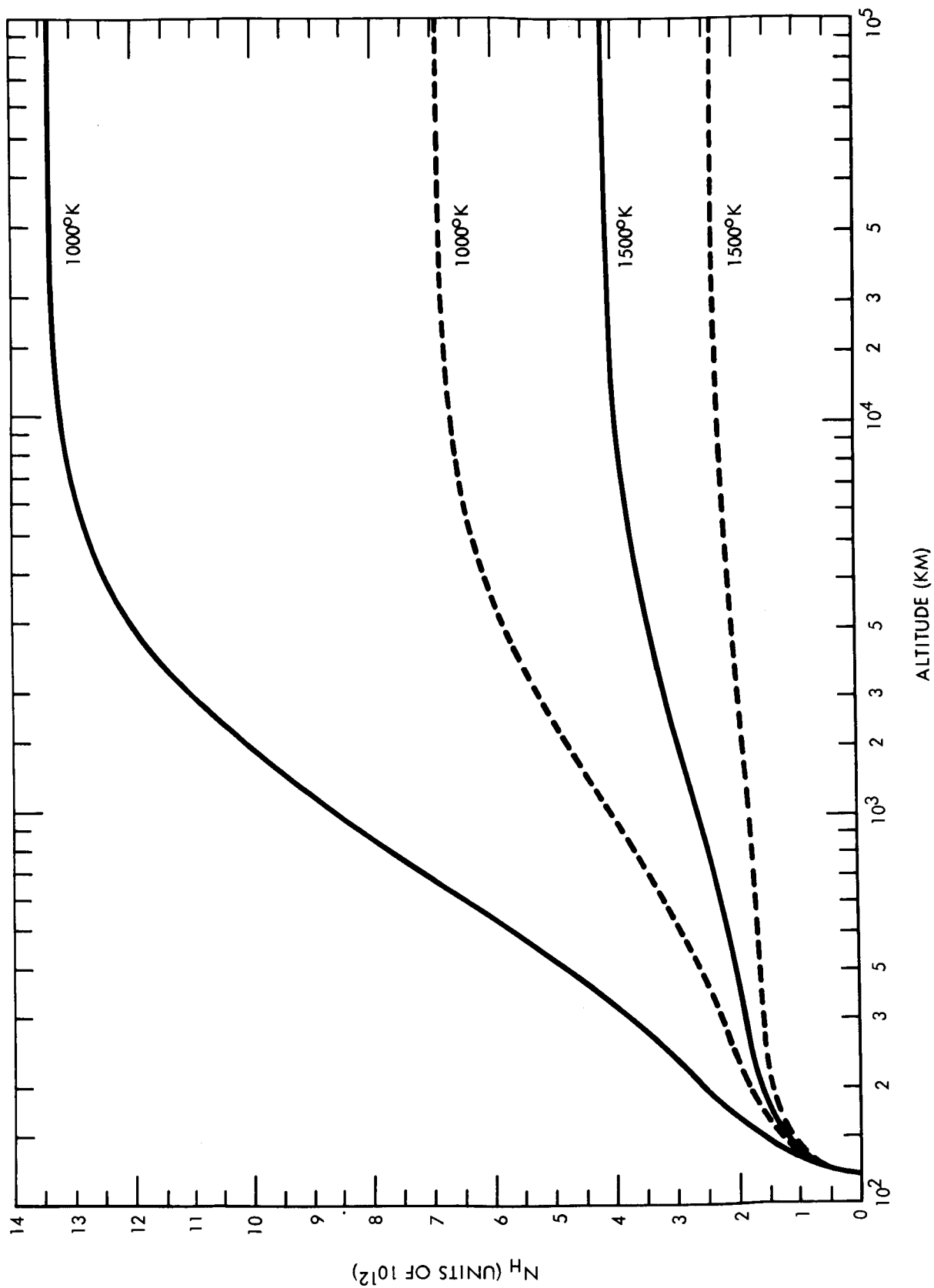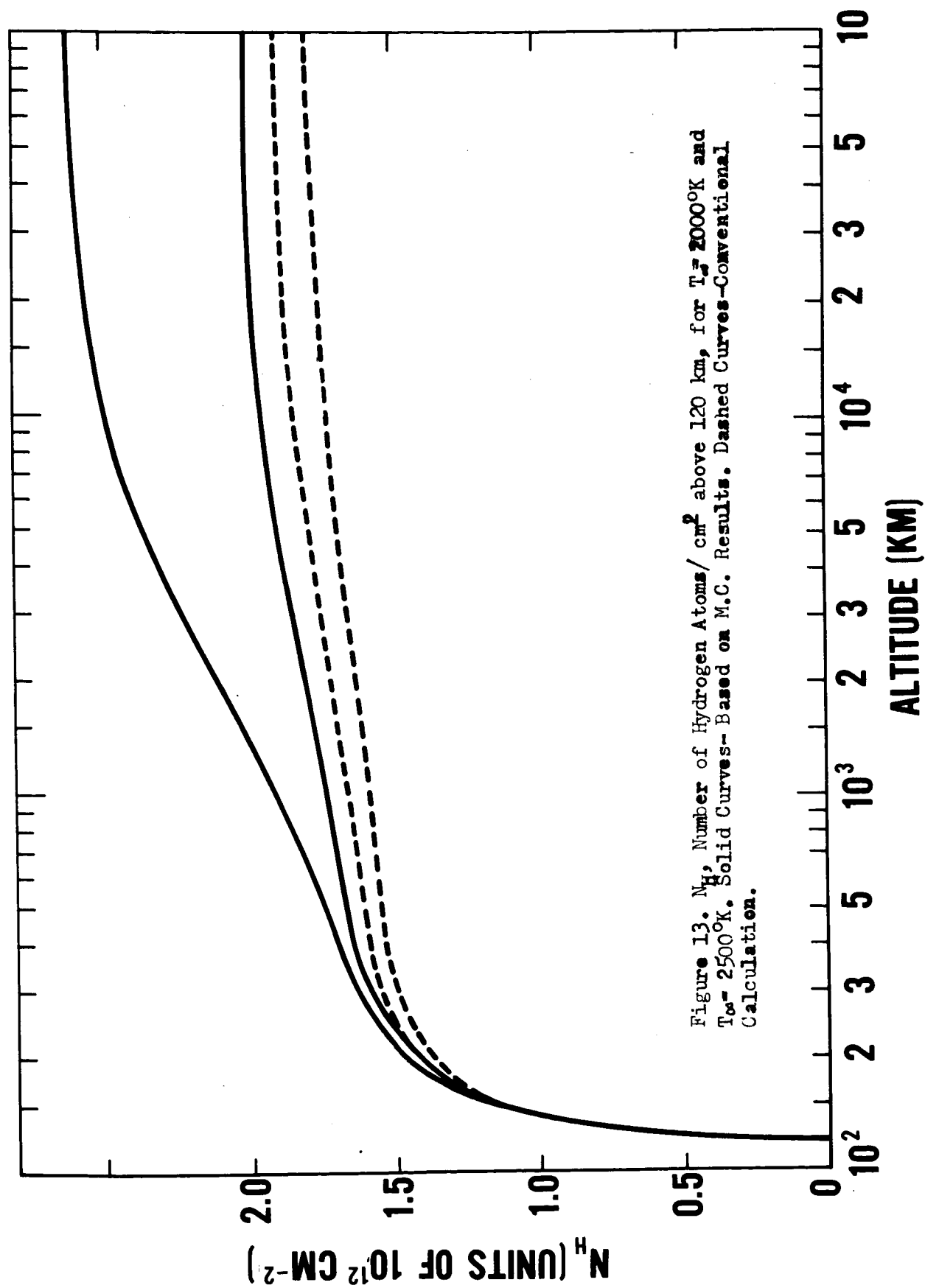
Figure 13. N_H, Number of Hydrogen Atoms/cm^2 above 120 km, for $T_s = 2000°K$ and $T_\infty = 2500°K$. Solid Curves–Based on M.C. Results. Dashed Curves–Conventional Calculation.